Cavity Balanced and Unbalanced Diplexer Based on Triple-Mode Resonator

Sai-Wai Wong, *Senior Member, IEEE*, Jing-Yu Lin, *Student Member, IEEE*, YangYang, *Senior Member, IEEE*, He Zhu, Rui-Sen Chen, *Student Member, IEEE*, Lei Zhu, *Fellow, IEEE*, and Yejun He, *Senior Member, IEEE*

***Abstract*—In this paper, a series of designs for cavity balanced and unbalanced diplexer are proposed. The balanced and unbalanced designs can be categorized into four groups—unbalanced-to-unbalanced, unbalanced-to-balanced, balanced-to-unbalanced (B2U), and balanced-to-balanced. First, two approaches to achieve out-of-phase characteristics of three fundamental modes, namely TE_{011}, TE_{101}, and TM_{110} in a single triple-mode resonator, are proposed for balun filter designs. Second, four types of unbalanced and balanced diplexers are presented by adopting these three fundamental modes, of which the Butterworth response applies with specific external quality and coupling coefficient. To the authors' best knowledge, full-metal cavity balun diplexer and balanced diplexer are not reported in the open literature. For proof of concept, the design of a B2U diplexer is fabricated and measured. Good matching between simulated and measured results shows the accuracy of the proposed design and methodology, which would be attractive in the high-power radio frequency (RF) front-end systems.**

***Index Terms*—Balanced diplexer, balun diplexer, balun filter, rectangular cavity, slot coupling, triple-mode resonator (TMR).**

I. Introduction

COMPARED with the single-ended circuits, balanced circuits contain lower environmental noise and even-order harmonic distortion so that they are widely applied in active and passive devices [1]–[3]. For one thing, the balun [4]–[8], as a key interface device, is the necessity for conversion between single-ended and balanced circuits. For another, the balanced filter [9]–[13], essential in increasing the signal-to-noise radio and efficiency, has the property of presenting the desired differential-mode response and suppressing common-mode signals. Both devices have been investigated using printed circuit boards (PCB) technologies [4]–[13]. Furthermore, to miniaturize the circuit volume and achieve multiple-function simultaneously, integration of several devices in one circuit is desired. The balun diplexer [14]–[17] and balanced diplexer [18]–[22], which integrate the diplexer and balun/balanced filter, have been fully investigated in PCB technologies [14]–[22]. In [15], the application of balun diplexers is explored in detail, and they can be divided into two categories 1) unbalanced-to-balanced (U2B) diplexer, which consists of one single-ended input and two pairs of balanced outputs and 2) balanced-to-unbalanced (B2U) diplexer, which is composed of a pair of balanced inputs and two single-ended outputs. Therefore, both single-ended and balanced signals can be achieved at input or outputs, respectively, of the diplexer.

Unfortunately, due to the Q-factor limitation, aforementioned balanced circuits implemented on the PCB process are not applicable in some application scenarios, where low insertion loss is required in narrow-band specifications. There are a few research works about the comprehensive studies on balanced and unbalanced cavity components according to the open literature. Generally, a cavity resonator is used in narrow-band system due to the high Q-factor, low insertion loss, and high selectivity. In [23], electromagnetically induced transparency (EMIT) filter is utilized to implement the unbalanced-to-unbalanced (U2U) filter/diplexer. In [24], the ceramic cavity is adopted to design a kind of single-ended diplexer with high isolation. In terms of cavity balun and balanced filters, Chen *et al*. [25]–[28] have made some progress in this field. In [25] and [26], a rectangular dielectric resonator is adopted to design the narrow-band balanced filters. In [27], the design of filtering balun is achieved by using $TE_{01\delta}$-mode dielectric resonator. In [28], the design of balun and balanced filters can be implemented simultaneously using dual-mode cross-shaped dielectric resonators. Besides, it is found in [17] that substrate integrated waveguide (SIW)-based balun diplexer and balanced diplexer are realized using the multilayer PCB process. Based on the authors' knowledge, there are no fully integrated metal cavity balun diplexer and balanced diplexer reported in the open literature.

In this paper, the phase characteristics of each fundamental mode are investigated, and two approaches to achieve out-of-phase characteristics are introduced. Four types of balanced

Manuscript received November 15, 2018; revised January 29, 2019 and May 20, 2019; accepted June 21, 2019. Date of publication July 17, 2019; date of current version February 10, 2020. This work was supported in part by the Shenzhen Science and Technology Programs under Grant JCYJ20180305124543176, in part by the Natural Science Foundation of Guangdong Province under Grant 2018A030313481, and in part by Shenzhen University Research Startup Project of New Staff under Grant 20188082. *(Corresponding author: Jing-Yu Lin.)*

S.-W. Wong, R.-S. Chen, and Y. He are with the College of Information Engineering, Shenzhen University, Shenzhen 518060, China (e-mail: wongsaiwai@ieee.org; 429889613@qq.com; heyejun@126.com).

J.-Y. Lin, Y. Yang, and H. Zhu are with the School of Electrical and Data Engineering, University of Technology Sydney, Ultimo, NSW 2007, Australia (e-mail: L.J.2014@ieee.org; yang.yang.au@ieee.org; he.zhu@uts.edu.au).

L. Zhu is with the Department of Electrical and Computer Engineering, University of Macau, Macau 999078, China (e-mail: leizhu@umac.mo).

Color versions of one or more of the figures in this paper are available online at http://ieeexplore.ieee.org

Digital Object Identifier 10.1109/TIE.2019.2928253

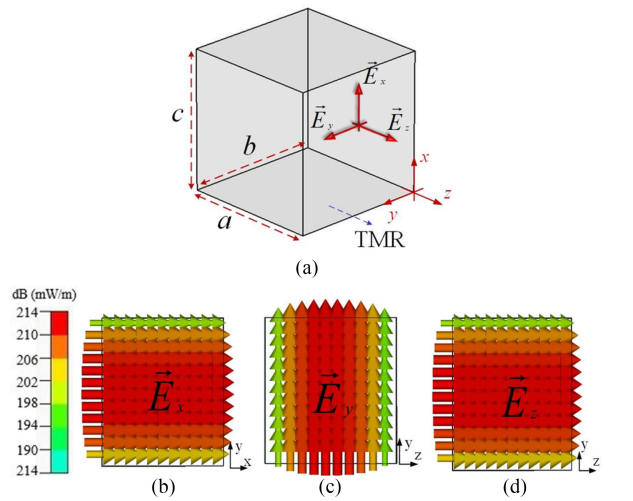

Fig. 1. (a) Three-dimensional physical model of a single TMR. (b)–(d) Electric field distributions of TE_{011}, TE_{101}, and TM_{110} modes, respectively.

and unbalanced diplexers are designed, and in order to achieve two out-of-phase fundamental modes simultaneously to design B2U and balanced-to-balanced (B2B) diplexers, the proposed two approaches are adopted at the input port at the same time. The advantages of the proposed structures compared with other traditional diplexers are summarized as follows:

1) Reduced circuit volume by sharing triple-mode resonator (TMR) resonator and omitting the matching network, and utilization of three fundamental modes also makes sure a compact cavity-based size.
2) Various single-ended or balanced inputs and outputs of diplexers can be achieved by adopting the introduced two approaches.

II. Implementation of Out-of-Phase Characteristics

Before presenting the balanced and unbalanced diplexer designs using three fundamental modes, the background knowledge of a triple-mode cavity resonator should be explored first. In [29], three fundamental modes are investigated, namely TE_{011}, TE_{101}, and TM_{110}, in a TMR cavity, of which the electric field directions are orthogonal to each other. The resonant frequencies of these modes can be determined by

$$\omega_{0,1,1}^2 = \frac{v^2}{\varepsilon_r u_r}\left[\left(\frac{\pi}{b}\right)^2 + \left(\frac{\pi}{c}\right)^2\right] \tag{1a}$$

$$\omega_{1,0,1}^2 = \frac{v^2}{\varepsilon_r u_r}\left[\left(\frac{\pi}{a}\right)^2 + \left(\frac{\pi}{c}\right)^2\right] \tag{1b}$$

$$\omega_{1,1,0}^2 = \frac{v^2}{\varepsilon_r u_r}\left[\left(\frac{\pi}{a}\right)^2 + \left(\frac{\pi}{b}\right)^2\right] \tag{1c}$$

where $\omega_{m,n,p}$ represents the resonant frequencies of the specific modes (m, n, and $p = 0$ or 1), and v represents the speed of light in the air. ε_r and μ_r are the permittivity and permeability of the air of the cavity, respectively. a, b, and c are the length, width, and height of a rectangular cavity, as depicted in Fig. 1(a), whose electric field distributions are depicted in Fig. 1(b)–(d).

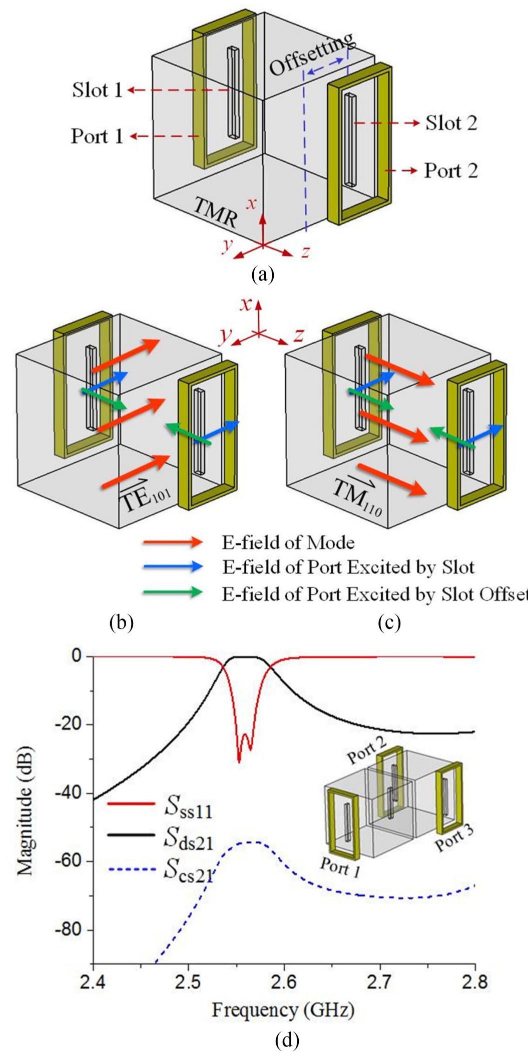

Fig. 2. (a) Three-dimensional view of TMR with off-center slots and ports. (b) Electric field distribution of TE_{101} mode. (c) Electric field distribution of TM_{110} mode. (d) Proposed second-order balun with differential-mode and common-mode transmission response.

Using (1a)–(1c), the resonant frequencies of the three fundamental modes can be controlled independently. The unloaded quality factors Q_u for these three modes are 20 204 for TE_{011} mode, 19 189 for TE_{101} mode, and 21 379 for TM_{110} mode, respectively.

Then, two approaches to achieve out-of-phase characteristics of three fundamental modes are proposed so that balanced ports of the balun and balanced diplexers can be achieved. Additionally, two balun filters are presented according to the proposed approaches.

A. Offsetting From Center

The first approach to achieve out-of-phase characteristic of each fundamental mode is that a pair of coupling slots are off-center, which is depicted in Fig. 2(a). A pair of symmetrical slots (slot 1 and slot 2) are located at off-center position versus the *xoy* plane, whose long-side orientation is perpendicular to the *y*-axis. Two electric-field directions $\vec{E}_z$ and $\vec{E}_y$ are produced to excite two fundamental modes: TM_{110} and TE_{101} [30]. Noticeably, port 1, port 2, and their respective coupling slots (slot 1 and slot 2) are absolutely symmetric, which means that port 1 and port 2 have the equivalent divided electromagnetic (EM) waves.

As depicted in Fig. 2(b), the electric field direction of TE_{101} (the red line) is consistent with electric field direction of two ports (the blue line in the y-axis direction), which means that the 0° phase imbalance will be achieved between two ports when TE_{101} mode is used. However, in Fig. 2(c), the electric field direction of TM_{110} (the red line) is only consistent with that of one port and reversed to the other port (the green line in the z-axis direction), so 180° phase imbalance will be achieved between two ports when TM_{110} mode is used. Therefore, one out-of-phase mode and one in-phase mode can be achieved in a single cavity using this approach.

In order to present the out-of-phase property and reflect the simulated results directly, a second-order balun filter adopting the off-center structure is proposed. Herein the mixed-mode S-parameters are used to present the differential-mode and common-mode transmission responses at the same time. The translation between three-port mixed-mode S-parameter and single-ended S-parameter is given in [15]

$$S_{ss11} = S_{11} \tag{2a}$$

$$S_{ds21} = \frac{1}{\sqrt{2}}(S_{21} - S_{31}) \tag{2b}$$

$$S_{cs21} = \frac{1}{\sqrt{2}}(S_{21} + S_{31}) \tag{2c}$$

where S_{ss11} is the return loss at the unbalanced port 1, S_{ds21} represents the two-port S-parameter from single-ended port 1 to balanced differential-mode port 2, and S_{cs21} is the two-port S-parameter from single-ended port 1 to balanced common-mode port 2, respectively.

Fig. 2(d) depicts the mixed-mode S-parameter curves of the proposed balun filter in the inset. It is deduced that it resonates at 2.57 GHz, which is dominated by TM_{110} mode. It has the 3-dB bandwidth of 50 MHz denoted in S_{ds21}, whereas the common-mode suppression denoted in S_{cs21} can reach 50 dB from 2.4 to 2.8 GHz.

B. Rotation at the Center

The second approach to achieve out-of-phase characteristic of each fundamental mode is that a pair of coupling slots are rotated at the center, which is depicted in Fig. 3(a). A pair of coupling slots (slot 1 and slot 2) etched on the surface versus the yoz plane of the cavity are crossed in respect to the center of the TMR cavity, where the energies are coupled with port 1 and port 2 evenly. Two electric field directions $\vec{E}_z$ and $\vec{E}_y$ are produced to excite two fundamental modes: TM_{110} and TE_{101} [30]. As depicted in Fig. 3(b), similar to the former approach, the electric field direction of TE_{101} (the red line) is consistent with that of two ports (the blue line in the y-axis direction). In Fig. 3(c), the electric field direction of TM_{110} (the red line) is only consistent with that of one port and reversed to the other port (the green line in the z-axis direction). Therefore, one out-of-phase mode and one in-phase mode are also achieved using this approach.

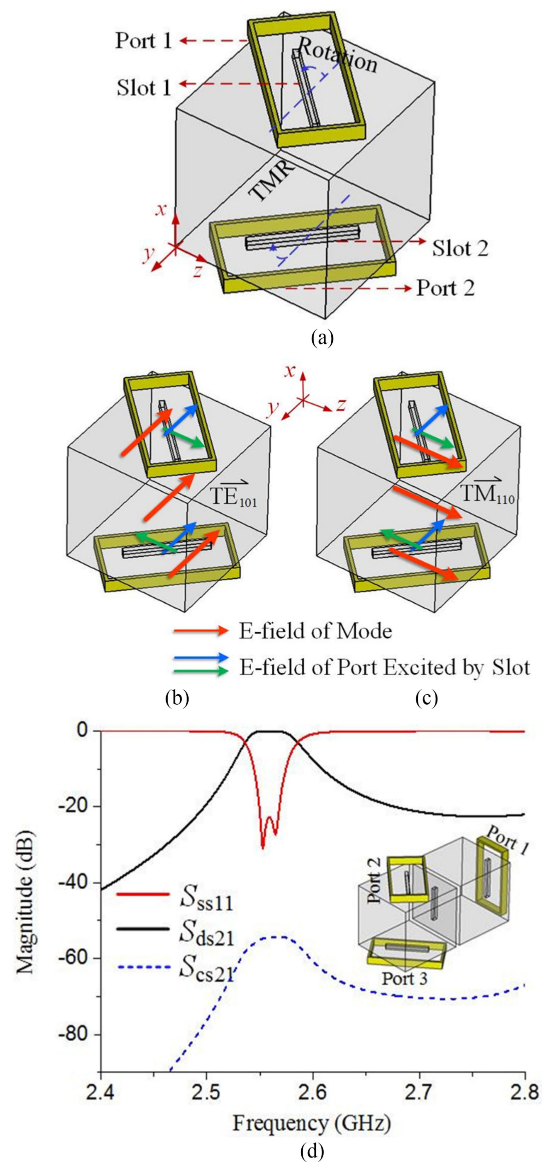

Fig. 3. (a) Three-dimensional view of TMR with rotated slots and ports. (b) Electric field distribution of TE_{101} mode. (c) Electric field distribution of TM_{110} mode. (d) Proposed second-order balun with differential-mode and common-mode transmission response.

Denoted in Fig. 3(d), the mixed-mode S-parameter results of the balun filter in the inset show that it resonates at 2.57 GHz, which is dominated by TM_{110} mode. Also, it has 3-dB bandwidth of 50 MHz denoted in S_{ds21}, and common-mode suppression of 50 dB and low differential-mode insertion loss are obtained.

In summary, in these two approaches, one out-of-phase mode and one in-phase mode are produced, simultaneously, while the out-of-phase mode can be utilized to achieve the balanced functions of the proposed diplexers.

Before starting to design balanced and unbalanced diplexers, the four-port mixed-mode S-parameters are presented here to express the differential-mode and common-mode transmission responses of the balanced filter. The translation between four-port mixed-mode S-parameter and single-ended S-parameter are

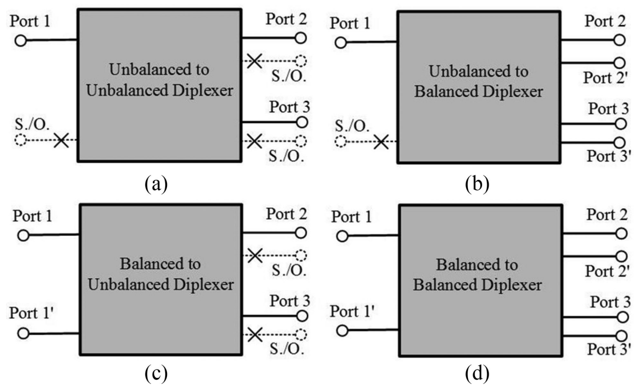

Fig. 4. Schematic diagram of four balanced and unbalanced diplexer couples.

given in [13]

$$S_{dd11} = \frac{(S_{11} - S_{1'1} - S_{11'} + S_{1'1'})}{2} \quad (3a)$$

$$S_{dd21} = \frac{(S_{21} - S_{2'1} - S_{21'} + S_{2'1'})}{2} \quad (3b)$$

$$S_{cc11} = \frac{(S_{11} + S_{1'1} + S_{11'} + S_{1'1'})}{2} \quad (3c)$$

$$S_{cc21} = \frac{(S_{21} + S_{2'1} + S_{21'} + S_{2'1'})}{2} \quad (3d)$$

where $S_{\mathrm{dd}11}$ is the return loss at the balanced differential-mode port 1, $S_{\mathrm{cc}11}$ is the return loss at the balanced common-mode port 1, $S_{\mathrm{dd}21}$ represents the two-port S-parameter from balanced differential-mode port 1 to port 2, and $S_{\mathrm{cc}21}$ is the two-port S-parameter from balanced common-mode port 1 to port 2.

III. Balanced and Unbalanced Diplexers

In previous section, we discuss two approaches to achieve out-of-phase characteristics of each of three fundamental modes in the structure. Herein we present four types of balanced and unbalanced diplexers, whose schematic diagrams are proposed in Fig. 4. As shown in Fig. 4(a), all three ports of the diplexer are single ended, which form up an U2U diplexer. In order to obtain the two balanced output ports, simultaneously, two more ports are added with totally four output ports. Hence, there are a single-ended input port 1 and two pairs of balanced output ports (port 2, port $2'$ and port 3, port $3'$) in the U2B diplexer schematic, as shown in Fig. 4(b). On the other hand, to achieve the balanced input ports (port 1 and port $1'$) and two single-ended output ports (port 2 and port 3), totally four ports are adopted to implement the B2U diplexer, as denoted in Fig. 4(c). For the implementation of all balanced input and output ports, simultaneously, there are six ports (port 1, port $1'$ for input, and port 2, port $2'$, port 3, port $3'$ for output) adopted to feed the B2B diplexer structure.

In the following diplexer designs, the uplink channel will be set to be dominated by TE_{011} mode, and the downlink channel will be set to be dominated by TM_{110} mode. Each channel of the diplexers is based on the synthesis design method with filtering response.

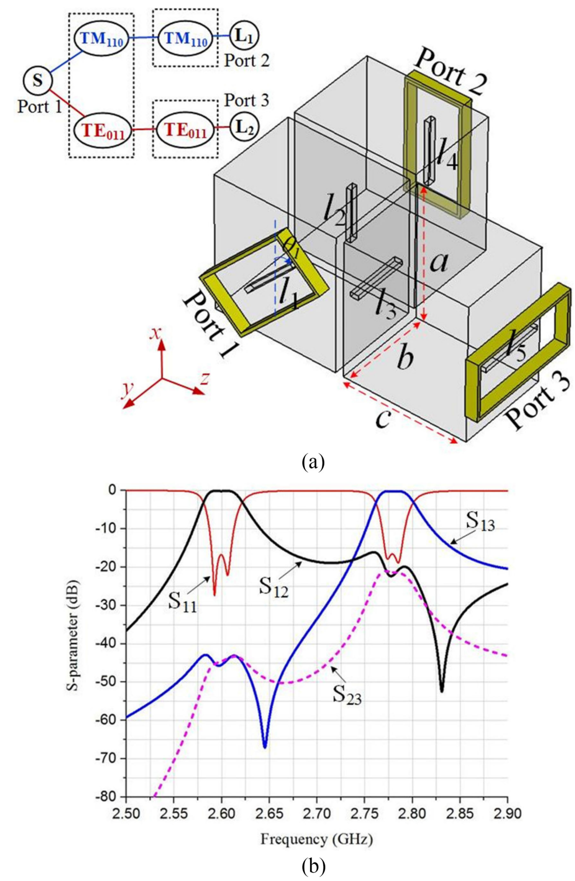

Fig. 5. U2U second-order diplexer with (a) physical structure and (b) simulated S-parameter curves.

A. U2U Diplexer

Fig. 5(a) depicts the physical model of the proposed U2U diplexer. A slot with length of l_1 rotates with an angle θ_1, and it excites two electric field orientations $\vec{E}_x$ and $\vec{E}_z$, which are in accordence with the directions of TE_{011} and TM_{110} modes. TE_{011} mode will be propagated into port 2, whereas TM_{110} mode will be propagated into port 3. The modal topology is given in the inset of Fig. 5(a).

Herein the filter synthesis method is then utilized to design the proposed diplexer. The fomula of external quality factors and coupling coefficients can be expressed as follows:

$$Q_e = \frac{g_0 g_1}{FBW} \quad (4a)$$

$$M_{12} = \frac{FBW}{\sqrt{g_1 g_2}} \quad (4b)$$

where g_0, g_1, and g_2 are the low-pass prototype element values of the second-order Butterworth polynomial, which can be set as $g_0 = 1$, $g_1 = g_2 = 1.4142$, and FBW is the fractional bandwidth.

Considering the specifications of the fractional bandwidths of 1.6% and 1.4% of two channels, the external quality factors

TABLE I
PHYSICAL DIMENSIONS OF THE DIPLEXER

a = 80 mm	b = 70 mm	c = 95 mm
θ_1 = 42 °	l_1 = 50 mm	l_2 = 39 mm
l_3 = 45 mm	l_4 = 45.4 mm	l_5 = 51.2 mm

and coupling coefficients can be calculated as follows:

$$Q_e^I = 90,\ Q_e^{II} = 98.3,\ M_{12}^I = 0.011,\ M_{12}^{II} = 0.010$$

Here Q_e^I, M_{12}^I and Q_e^{II}, M_{12}^{II} are the values of first and second channels of the proposed diplexer, respectively.

The relationships between the coupling coefficients and external quality factors based on the physical model dimensions of coupled resonators can be extracted according to [31]

$$M_{ij} = \pm\frac{f_{p2}^2 - f_{p1}^2}{f_{p2}^2 + f_{p1}^2} \tag{5a}$$

$$Q_e = \frac{f_0}{\Delta f_{3-dB}} \tag{5b}$$

where f_{p1} and f_{p2} are the resonant frequencies of the two coupled resonators, f_0 stands for the center frequency, and $\Delta f_{3-\mathrm{dB}}$ stands for bandwidths between $\pm 90°$ phase offsettings of the resonant frequency.

It can be seen in Fig. 5(b) that TE_{011} mode resonates at 2.6 GHz with 3-dB bandwidth of 41 MHz denoted in S_{12}, whereas TM_{110} mode resonates at 2.78 GHz with 3-dB bandwidth of 40 MHz denoted in $|S_{13}|$. The isolation between port 2 and port 3 can reach 25 dB from 2.5 to 2.9 GHz.

The physical dimensions of the proposed U2U diplexer are tabulated in Table I. The width and thickness of all the coupling slots are 3 and 5mm, respectively.

B. U2B Diplexer

Balun diplexer can be categoried as U2B diplexer and B2U diplexer. According to the analysis of two approaches in Section II, to implement U2B's property, one out-of-phase mode and one in-phase mode will be achieved at each of two outputs of the diplexer, as depicted in the inset of Fig. 6(a). The physical structure of the U2B diplexer processes one single-ended input port 1 and two pairs of balanced output ports (port 2, port 2′ and port 3, port 3′) working at different channels, respectively. A slot with the length of l_6 rotates with an angle $\theta_{2,}$ and it excites two electric field orientations $\vec{E}_x$ and $\vec{E}_z$, which are in accordence with the directions of TE_{011} and TM_{110} modes. TE_{011} mode will be propagated into a pair of balanced ports (port 2 and port 2′) whereas TM_{110} mode into another pair of balanced ports (port 3 and port 3′). The "offsetting from center" approach in Fig. 2(a) is adopted here; the coupling slots with the length l_{10} are off-center versus the *yoz* plane, and their long-side orientations are perpendicular to the *y*-axis, so that the EM waves of out-of-phase TE_{011} mode and in-phase TE_{101} mode would be evenly transmitted into port 3 and port 3′ due to the symmetrical structure. Similarly, The "rotation at the center" approach in Fig. 3(a) is adopted at the other pair of outputs, and a pair of slots with length of l_9 make a cross versus the *yoz* plane; it means that the EM waves of out-of-phase TM_{110} mode and in-phase TE_{101} mode would propagate through port 2 and port 2′, evenly.

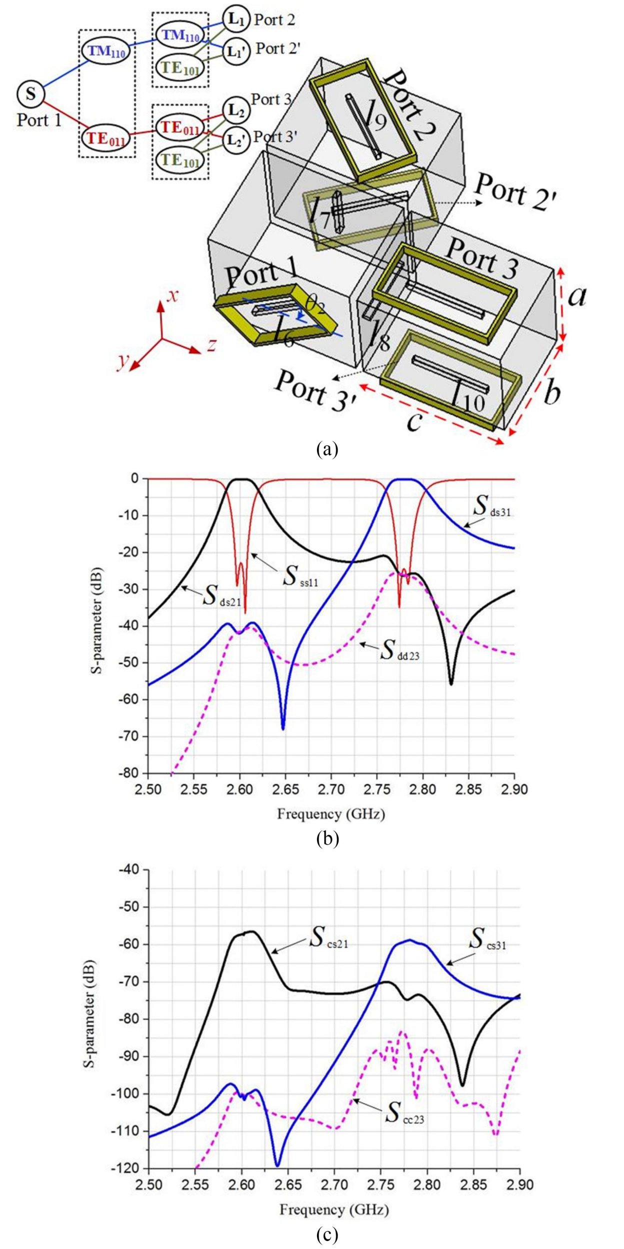

Fig. 6. U2U second-order diplexer with (a) physical structure, (b) differential-mode response, and (c) common-mode response.

To obtain a well-designed balun diplexer, both channels need to meet the required external quality factors and coupling coefficients versus function response according to [15] as follows:

$$Q_e^s = Q_e^d = \frac{g_0 g_1}{FBW} \tag{6a}$$

$$M_{12} = \frac{FBW}{\sqrt{g_1\, g_2}} \tag{6b}$$

where Q_e^s and Q_e^d are the external quality factors of a single-ended port and a differential-mode port, respectively.

TABLE II
PHYSICAL DIMENSIONS OF THE DIPLEXER

a = 80 mm	b = 70 mm	c = 95 mm
θ_2 = 42 °	l_6 = 50 mm	l_7 = 39.2 mm
l_8 = 43.8 mm	l_9 = 47.4 mm	l_{10} = 50 mm

In this case, considering the specifications of the fractional bandwidths of 1.4% and 1.6% of two channels, the external quality factors and coupling coefficients can be calculated as follows:

$$Q_e^{sI} = Q_e^{dI} = 101,\ Q_e^2 = Q_e^{2'} = 2\,Q_e^{dI} = 202,\ M_{12}^I = 0.0099,$$
$$Q_e^{sII} = Q_e^{dII} = 88,\ Q_e^3 = Q_e^{3'} = 2\,Q_e^{dII} = 176,\ M_{12}^{II} = 0.011.$$

Here Q_e^{sI} and Q_e^{sII} are the external quality factors of first and second channels of the input port 1, and Q_e^2, $Q_e^{2'}$, and Q_e^3, $Q_e^{3'}$ are the external quality factors of two pairs of balanced ports (port 2, port 2′ and port 3, port 3′).

Fig. 6(b) and (c) shows the mixed-mode S-parameters of the U2B diplexer. Followed by formulas (2a)–(2c), it can be seen in Fig. 6(b) for differential-mode response that TE_{011} mode resonates at 2.6 GHz with 3-dB bandwidth of 36 MHz denoted in S_{ds21} , whereas TM_{110} mode resonates at 2.78 GHz with 3-dB bandwidth of 45 MHz denoted in S_{ds31} due to the fact that TE_{101} mode is an in-phase mode, which is not resonated within the frequency range. The isolation between two balanced ports denoted in S_{dd23} can reach 24 dB from 2.8 to 3.2 GHz. In Fig. 6(c) the common-mode suppression of TE_{011} mode can reach 55 dB denoted in S_{cs21} while that of TM_{110} mode denoted in S_{cs31} is 60 dB, and the common-mode isolation between the two balanced output ports denoted in S_{cc23} can reach 80 dB.

The physical dimensions of the proposed U2B diplexer are tabulated in Table II. The width and thickness of all the coupling slots are 3 and 5 mm, respectively.

C. B2U Diplexer

In former case, we have discussed the design of the U2B diplexer, herein there is one of the balun diplexers still imperative: the B2U diplexer. Its schematic is proposed in Fig. 4(c). This type of diplexer is composed of a pair of balanced input ports and two single-ended output ports for transmitting/receiving. It is noted that to achieve balun function in both channels of the diplexer, we need to achieve two out-of-phase modes simultaneously at the input ports, as illustrated in the inset of Fig. 7(a). Therefore, the “offsetting from center” and “rotation at the center” approaches are combined to produce two out-of-phase modes, as illustrated in Fig. 7(b), and a pair of coupling slots make a cross with offsetting along the y-axis, which can be divided into the following two parts:

1) Making a cross at the center excites the reversed electric field $\vec{E}_z$ with out-of-phase TM_{110} mode.
2) Offsetting away the center position excites the reversed electric field $\vec{E}_x$ with out-of-phase TE_{011} mode.

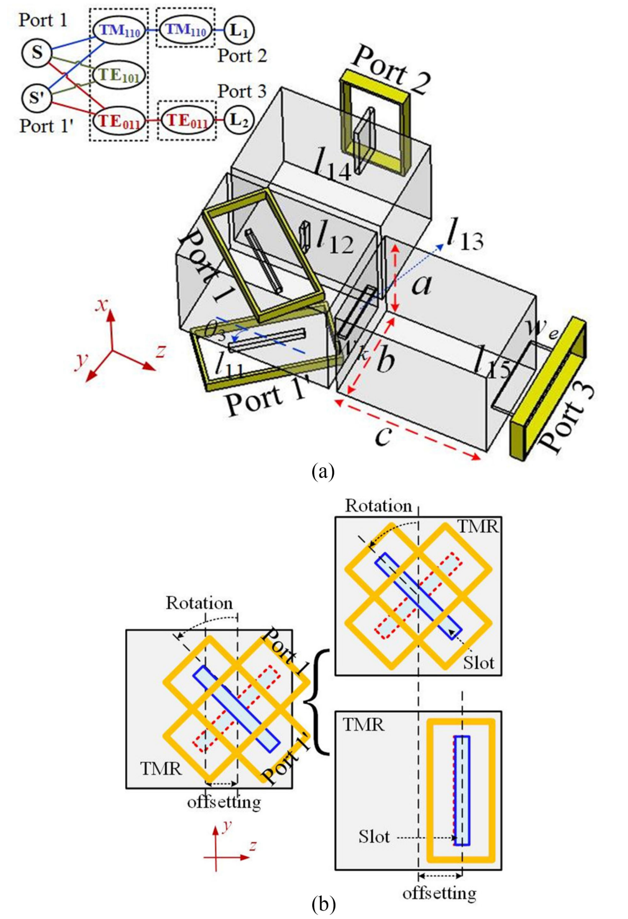

Fig. 7. B2U second-order diplexer with (a) physical structure, (b) electric field analysis.

Therefore, in the physical structure of B2U second-order diplexer in Fig. 7(a), a pair of slots with the length of l_{11} are coupled from the balanced ports (port 1 and port 1′) and excite the out-of-phase TE_{011} and TM_{110} modes simultaneously; TM_{110} mode propagates into single-ended port 2, whereas TE_{011} mode propagates into single-ended port 3. Formulas (6a)–(6b) are also utilized to calculate the required external quality factors and coupling coefficients of each band.

In this case, considering the specifications of the fractional bandwidths of 1.1% and 1.5% of two channels, the external quality factors and coupling coefficients can be calculated as follows:

$$Q_e^{sI} = Q_e^{dI} = 123.3,\ Q_e^{1I} = Q_e^{1'I} = 2\,Q_e^{dI} = 246.6,$$
$$M_{12}^I = 0.008, Q_e^{sII} = Q_e^{dII} = 91.4,$$
$$Q_e^{1II} = Q_e^{1'II} = 2\,Q_e^{dII} = 182.8,\ M_{12}^{II} = 0.011.$$

Here Q_e^{sI} and Q_e^{sII} are the external quality factors of first and second channels of the output port 2 and port 3, Q_e^{1I}, $Q_e^{1'I}$ and Q_e^{1II}, $Q_e^{1'II}$ are the external quality factors of two channels of the balanced ports (port 1 and port 1′).

In [29], how to extract the Q_e and M_{12} based on the physical dimensions of coupled resonators is presented in detail. Due

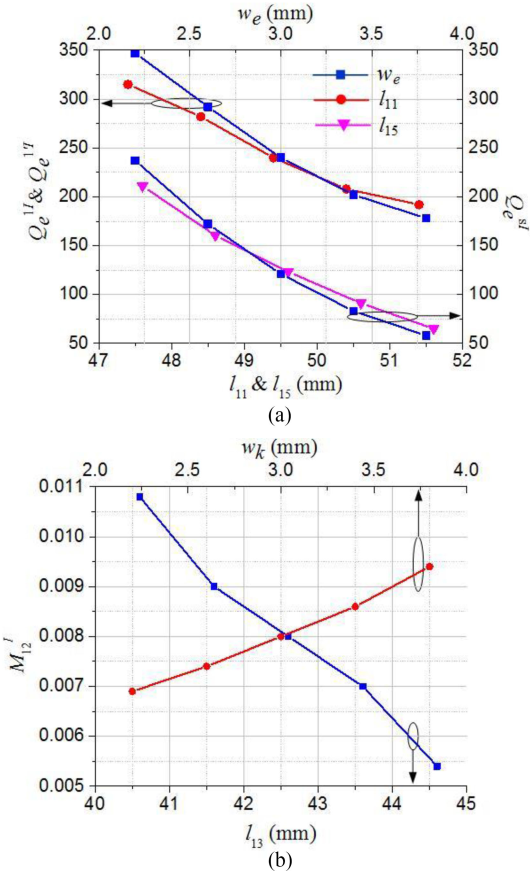

Fig. 8. Variation trend versus varied physical parameters. (a) External quality factor Q_e^{1I}, $Q_e^{1'I}$, and Q_e^{sI}. (b) Coupling coefficient M_{12}^I.

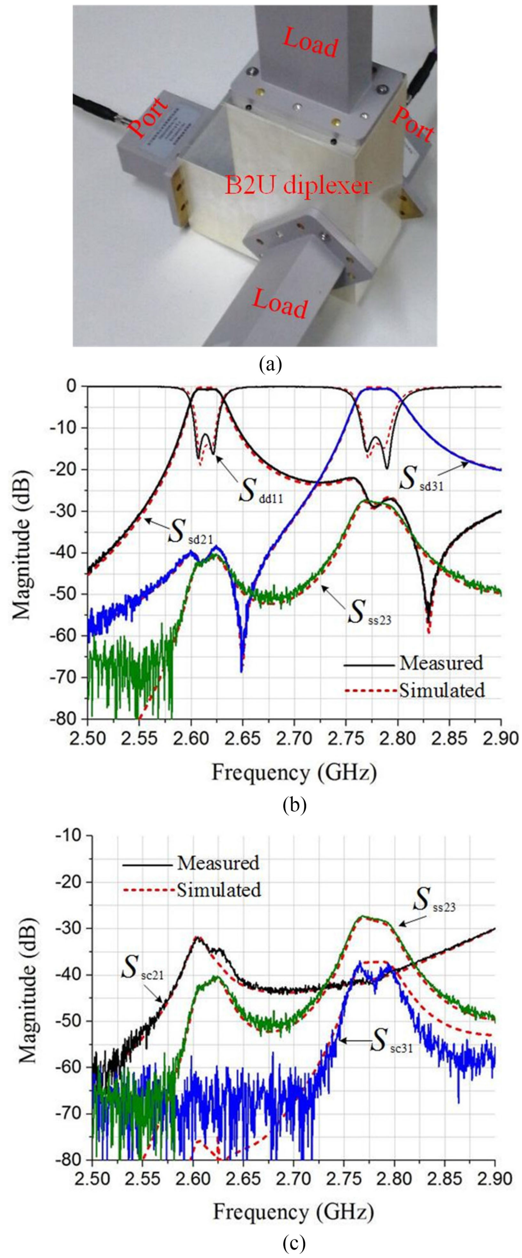

Fig. 9. (a) Working state of the fabricated B2U diplexer structure. Compared simulated and measured results with (b) differential-mode response and (c) common-mode response.

to the reciprocity for three fundamental modes, TE_{011} mode is used as an example to provide the variation trend of Q_e^{1I}, Q_e^{sI}, and M_{12}^I versus varied physical parameters, as shown in Fig. 8. By properly setting the suitable values specified in Fig. 8(a) and (b), the prescribed Q_e^{1I}, Q_e^{sI}, and M_{12}^I can be achieved to meet the required filtering response.

The structure of B2U diplexer is fabricated to verify the accuracy of the proposed design methodology. Fig. 9(a) shows the working state of the fabricated B2U diplexer structure. Silver plated aluminum is the material for fabricating the proposed full-metal cavity diplexer using computer numerical control technology. WR284-type rectangular waveguides are used to feed the ports. Fig. 9(b) and (c) shows the compared simulated and measured mixed-mode *S*-parameter results of this structure. Followed by formulas (2a)–(2c), it can be seen in Fig. 9(b) for differential-mode response that TE_{011} mode resonates at 2.61 GHz with 3-dB bandwidth of 30 MHz and measured insertion loss of 0.7 dB denoted in $S_{\mathrm{sd}21}$, whereas TM_{110} mode resonates at 3.11 GHz with 3-dB bandwidth of 43 MHz and measured insertion loss of 0.6 dB denoted in $S_{\mathrm{sd}31}$. The achieved unloaded *Q* factor Q_u can be calculated as 1843 at 2.61 GHz channel and 1598 at 2.78 GHz channel compared with the expected Q_u of 3225 at 2.61 GHz channel and 2397 at 2.78 GHz channel. The isolation between port 2 and port 3 denoted in $S_{\mathrm{ss}23}$ can reach 27 dB from 2.5 to 2.9 GHz. In Fig. 9(c), the common-mode suppression of TE_{011} mode can reach 32 dB while that of TM_{110} mode is 38 dB.

TABLE III
PHYSICAL DIMENSIONS OF THE DIPLEXER

a = 80 mm	b = 70 mm	c = 95 mm
θ_3 = 40 °	l_{11}= 50.4 mm	l_{12}= 39.4 mm
l_{13} = 42.6 mm	l_{14} = 45.4 mm	l_{15} = 49.6 mm

The physical dimensions of the proposed U2B diplexer are tabulated in Table III. The width of all the coupling slots are 3 mm.

TABLE IV
COMPARISON BETWEEN THE BALUN DIPLEXER AND OTHER REPORTED ONES

	Implemented Meterial	Central Frequency	Frequency Ratio	Achieved Bandwidths	Measured Insertion Loss	Filtering Order	Achieved Isolation	Common-mode Rejection
[15]	PCB (Planar)	1.85/2.45	1.32	11.1/9.3	1.42/1.77	3	33 dB	33 dB
[17]	PCB (SIW)	2.2/2.8	1.27	2.7/1.7	2.2/2.7	2	28 dB	44 dB
This work	Metal Cavity	2.61/2.78	1.06	1.1/1.5	0.7/0.6	2	27 dB	32 dB

The comparison between the fabricated B2U diplexer and other reported ones is presented in Table IV. According to Table IV, it is clear that under the circumstance of high isolation and common-mode rejection, our design can achieve a low frequency ratio of only 1.06 due to the utilization of fundamental orthogonal modes. It means that two channels of the diplexer can be designed closer without severe deterioration of isolation. Additionally, lower insertion loss is also obtained. It is noteworthy that the reported work in [15] has a better isolation due to the higher filtering order (third order) and wider frequency ratio.

D. B2B Diplexer

Balanced diplexer consists of a pair of balanced input ports (port 1 and port 1′) and two pairs of balanced output ports (port 2, port 2′ and port 3, port 3′). Therefore, it combines the balanced inputs in B2U diplexer and two pairs of balanced outputs in U2B diplexer. The modal topology and the physical structure are presented in Fig. 10(a). A pair of coupling slots make a cross with offsetting along the y-axis, so that the out-of-phase TE_{011} and TM_{110} modes are excited simultaneously. The EM waves of TE_{011} mode propagate into a pair of balanced outputs (port 3 and port 3′), due to the fact that port 3 and port 3′ also make a cross to absorb the EM waves of TE_{011} mode. Similarly, the EM waves of TM_{110} mode pour into another balanced outputs (port 2 and port 2′). Therefore, because of the modal orthogonality between TE_{011} and TM_{110} modes, excellent isolation can be obtained in this balanced diplexer.

To obtain a well-designed balanced diplexer, both channels need to meet the required external quality factors and coupling coefficients versus function response according to [28] as follows:

$$Q_e^d = \frac{g_0 g_1}{FBW} \tag{7a}$$

$$M_{12} = \frac{FBW}{\sqrt{g_1\, g_2}}. \tag{7b}$$

In this case, considering the specifications of the fractional bandwidths of 1.2% and 1.6% of two channels, the external quality factors and coupling coefficients can be calculated as follows:

$$Q_e^{dI} = 115.3,\ Q_e^{1I} = Q_e^{1'I} = Q_e^2 = Q_e^{2'} = 2\,Q_e^{dI} = 230.6,$$
$$M_{12}^I = 0.009,\ Q_e^{dII} = 87.3,\ Q_e^{1II} = Q_e^{1'II} = Q_e^3 = Q_e^{3'}$$
$$= 2\,Q_e^{dII} = 174.6,\ M_{12}^{II} = 0.011.$$

Here Q_e^{1I}, $Q_e^{1'I}$ and Q_e^{1II}, $Q_e^{1'II}$ are the external quality factors of two channels of the balanced ports (port 1 and port 1′). Q_e^2, $Q_e^{2'}$ and Q_e^3, $Q_e^{3'}$ are the external quality factors of two pairs of balanced ports (port 2, port 2′ and port 3, port 3′).

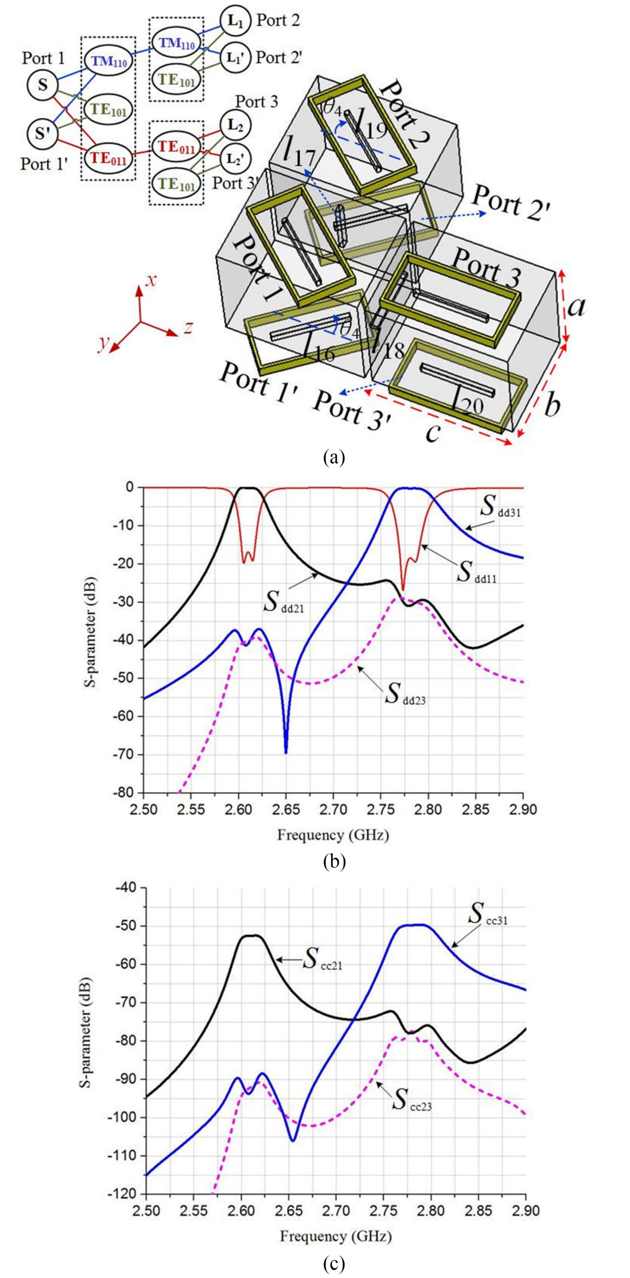

Fig. 10. B2B second-order diplexer with (a) physical structure, (b) differential-mode response, and (c) common-mode response.

Fig. 10(b) and (c) shows the mixed-mode S-parameters of the balanced diplexer. It can be seen in Fig. 10(b) for

TABLE V
PHYSICAL DIMENSIONS OF THE DIPLEXER

a = 80 mm	b = 70 mm	c = 95 mm
θ_4 = 40°	l_{16} = 50.8 mm	l_{17} = 39.6 mm
l_{18} = 43 mm	l_{19} = 47.2 mm	l_{20} = 48.8 mm

differential-mode response that TE_{011} mode resonates at 2.61 GHz with 3-dB bandwidth of 32 MHz denoted in S_{dd21}, whereas TM_{110} mode resonates at 2.78 GHz with 3-dB bandwidth of 45 MHz denoted in S_{dd31}. The differential-mode isolation between two pairs of balanced output ports denoted in S_{dd23} can reach 25 dB from 2.5 to 2.9 GHz. In Fig. 8(c), the common-mode suppression of TE_{011} mode can reach 50 dB while that of TM_{110} mode is 45 dB. The common-mode isolation is higher than 75 dB among the frequency range.

The physical dimensions of the proposed B2B diplexer are tabulated in Table V. The width of all the coupling slots are 3 mm.

IV. CONCLUSION

In this paper, we proposed and summarized all couples of balanced and unbalanced diplexers. Also, the design methodology of these devices were fully investigated. All the designs are implemented by adopting three fundamental modes, namely TE_{011}, TE_{101}, and TM_{110}, of the TMRs, of which the Butterworth response applies with specific external quality and coupling coefficient. The structure of B2U diplexer was fabricated to verify the accuracy of the proposed design methodology. The proposed designs have the potential values in the high-power radio frequency (RF) front-ends, as the transformers between single-ended/differential antennas and single-ended/differential transmitter/receiver. The achieved low-frequency ratio is promising in some required adjacent-channel diplexers.

REFERENCES

[1] F. Lin, “A planar balanced quadrature coupler with tunable power-dividing ratio,” *IEEE Trans. Ind. Electron*, vol. 65, no. 8, pp. 6515–6526, Aug. 2018.

[2] R. Quaglia and S. Cripps, “A load modulated balanced amplifier for telecom applications,” *IEEE Trans. Microw. Theory Techn.*, vol. 66, no. 3, pp. 1328–1338, Mar. 2018.

[3] B. Li and K. W. Leung, “On the differentially fed rectangular dielectric resonator antenna,” *IEEE Trans. Antennas Propag.*, vol. 56, no. 2, pp. 353–359, Feb. 2008.

[4] E.-Y. Jung and H.-Y. Hwang, “A balun-BPF using a dual mode ring resonator,” *IEEE Microw. Wireless Compon. Lett.*, vol. 17, no. 9, pp. 652–654, Sep. 2007.

[5] L. K. Yeung and K.-L. Wu, “A dual-band couple-line balun filter,” *IEEE Trans. Microw. Theory Techn.*, vol. 55, no. 11, pp. 2406–2411, Nov. 2007.

[6] C.-H. Wu, C.-H. Wang, S.-Y. Chen, and C. H. Chen, “Balanced-to-unbalanced bandpass filters and the antenna application,” *IEEE Trans. Microw. Theory Techn.*, vol. 56, no. 11, pp. 2474–2482, Nov. 2008.

[7] Z.-Y. Zhang and K. Wu, “A broadband substrate integrated waveguide (SIW) planar balun,” *IEEE Microw. Wireless Compon. Lett.*, vol. 17, no. 12, pp. 843–845, Dec. 2007.

[8] L.-S. Wu, Y.-X. Guo, J.-F. Mao, and W.-Y. Yin, “Design of a substrate integrated waveguide balun filter based on three-port coupled-resonator circuit model,” *IEEE Microw. Wireless Compon. Lett.*, vol. 21, no. 5, pp. 252–254, May 2011.

[9] C.-H. Wu, C.-H. Wang, and C. H. Chen, “Novel balanced coupled-line bandpass filters with common-mode noise suppression,” *IEEE Trans. Microw. Theory Techn.*, vol. 55, no. 2, pp. 287–295, Feb. 2007.

[10] C.-H. Wu, C.-H. Wang, and C. H. Chen, “Balanced coupled-resonator bandpass filters using multisection resonators for common-mode suppression and stopband extension,” *IEEE Trans. Microw. Theory Techn.*, vol. 55, no. 8, pp. 1756–1753, Aug. 2007.

[11] T. B. Lim and L. Zhu, “A differential-mode wideband bandpss filter on microstrip line for UWB application,” *IEEE Microw. Wireless Compon. Lett.*, vol. 19, no. 10, pp. 632–634, Oct. 2009.

[12] T. B. Lim and L. Zhu, “Highly selective differential-mode wideband bandpass filter for UWB applcation,” *IEEE Microw. Wireless Compon. Lett.*, vol. 21, no. 3, pp. 133–135, Mar. 2011.

[13] W. Feng and W. Che, “Novel wideband differential bandpass filters based on T-shaped structure,” *IEEE Trans. Microw. Theory Techn.*, vol. 60, no. 6, pp. 1560–1568, Jun. 2012.

[14] C.-H. Wu, C.-H. Wang, and C. H. Chen, “A novel balanced-to-unbalanced diplexer based on four-port balanced-to-balanced bandpass filter,” presented at the 2008 38th Eur. IEEE Micro. Conf., Amsterdam, Netherlands, Oct. 2008, pp. 28–31.

[15] Q. Xue, J. Shi, and J.-X. Chen, “Unbalanced-to-balanced and balanced-to-unbalanced diplexer with high selectivity and common-mode suppression,” *IEEE Trans. Microw. Theory Techn.*, vol. 59, no. 11, pp. 2848–2855, Nov. 2011.

[16] P.-L. Chi and T. Yang, “Novel 1.5-2.4 GHz tunable single-to-balanced diplexer,” *IEEE Microw. Wireless Compon. Lett.*, vol. 26, no. 10, pp. 783–785, Oct. 2016.

[17] M. F. Hagag, M. A. Khater, M. D. Hickle, and D. Peroulis, “Tunable SIW cavity-based dual-mode diplexers with various single-ended and balanced ports,” *IEEE Trans. Microw. Theory Techn.*, vol. 66, no. 3, pp. 1238–1248, Mar. 2018.

[18] Z.-H. Bao, J.-X. Chen, E. H. Lim, and Q. Xue, “Compact microstrip diplexer with differential outputs,” *Electron. Lett.*, vol. 46, no. 11, pp. 766–768, May 2010.

[19] Y. Zhou, H.-W. Deng, and Y. Zhao, “Compact balanced-to-balanced microstrip diplexer with high isolation and common-mode suppression,” *IEEE Microw. Wireless Compon. Lett.*, vol. 24, no. 3, pp. 143–145, Mar. 2014.

[20] X. Guo, L. Zhu, and W. Wu, “Balanced dipexers based on inner-coupled dual-mode structure with intrinsic common-mode suppression,” *IEEE Access*, vol. 5, pp. 26774–26782, Nov. 2017.

[21] A. Fernandez-Prieto *et al.*, “Compact balanced-to-balanced diplexer based on split-ring resonators balanced bandpass filters,” *IEEE Microw. Wireless Compon. Lett.*, vol. 28, no. 3, pp. 218–220, Mar. 2018.

[22] A. Fernandez-Prieto *et al.*, “Balanced-to-balanced microstrip diplexer based on magnetically coupled resonators,” *IEEE Access*, vol. 6, pp. 18536–18547, Mar. 2018.

[23] X. Q. Lin, J. Y. Jin, J. W. Yu, Y. Jiang, Y. Fan, and Q. Xue, “Design and analysis of EMIT filter and diplexer,” *IEEE Trans. Ind. Electron*, vol. 64, no. 4, pp. 3059–3066, Apr. 2017.

[24] D. Hendry and A. Abbosh, “Compact high isolation base-station duplexer using triple-mode ceramic cavities,” *IEEE Trans. Ind. Electron*, vol. 65, no. 10, pp. 8092–8100, Oct. 2018.

[25] J.-X. Chen, Y. Zhan, W. Qin, Z.-H. Bao, and Q. Xue, “Novel narrow-band balanced bandpass filter using rectangular dielectric resonator,” *IEEE Microw. Wireless Compon. Lett.*, vol. 25, no. 5, pp. 289–291, May 2015.

[26] J.-X. Chen, Y. Zhan, W. Qin, Z.-H. Bao, and Q. Xue, “Analysis and design of balanced dielectric resonator bandpass filter,” *IEEE Trans. Microw. Theory Techn.*, vol. 64, no. 5, pp. 1476–1483, May 2016.

[27] J.-X. Chen, Y. Zhan, W. Qin, and Z.-H. Bao, “Design of high-performance filtering balun based on TE01δ-mode dielectric resonator,” *IEEE Trans. Ind. Electron*, vol. 64, no. 1, pp. 451–458, Jan. 2017.

[28] J.-X. Chen, J. Li, Y. Zhan, W. Qin, J. Shi, and Z.-H. Bao, “Design of balanced and balun filters using dual-mode cross-shaped dielectric resonators,” *IEEE Trans. Microw. Theory Techn.*, vol. 65, no. 4, pp. 1226–1234, Apr. 2017.

[29] J.-Y. Lin, S.-W. Wong, L. Zhu, and Q.-X. Chu, “Design of miniaturized triplexers via sharing a single triple-mode cavity resonator,” *IEEE Trans. Microw. Theory Techn.*, vol. 65, no. 10, pp. 3877–3884, Oct. 2017.

[30] Z.-C. Guo *et al.*, “Triple-mode cavity bandpass filter on doublet with controllable transmission zeros, ” *IEEE Access*, vol. 5, pp. 6969–6977, Apr. 2017.

[31] J. S. Hong and M. J. Lancaster, *Microstrip Filters for RF/Microwave Applications*. New York, NY, USA: Wiley, 2001.

Sai-Wai Wong (S'06–M'09–SM'14) received the B.S. degree in electronic engineering from the Hong Kong University of Science and Technology, Hong Kong, in 2003, and the M.Sc. and Ph.D. degrees in communication engineering from Nanyang Technological University, Singapore, in 2006 and 2009, respectively.

From 2003 to 2005, he was the Lead Engineering Department in mainland of China, with two Hong Kong manufacturing companies. From 2009 to 2010, he was a Research Fellow with the Institute for Infocomm Research, Singapore. In 2010, he was an Associate Professor and became a Full Professor with the School of Electronic and Information Engineering, South China University of Technology, Guangzhou, China. In 2016, he was a Visiting Professor with the City University of Hong Kong. In 2017, he was a Visiting Professor with the University of Macau. Since 2017, he has been a Full Professor with the College of Electronic and Information Engineering, Shenzhen University, Shenzhen, China. His current research interests include RF/microwave circuit and antenna design. He is a Reviewer for several top-tier journals.

Dr. Wong was a recipient of the New Century Excellent Talents in University Award in 2013 and the Shenzhen Overseas High-Caliber Personnel Level C in 2018.

Jing-Yu Lin (S'14) received the B.E. degree from Southwest Jiaotong University, Chengdu, China, in 2016, and the M.E. degree from the School of Electronic and Information Engineering, South China University of Technology, Guangzhou, China, in 2018. He is currently working toward the Ph.D. degree with the University of Technology Sydney, Ultimo, NSW, Australia.

From 2017 to 2019, he was as an exchange student in the University of Technology Sydney. His current research interests include microwave cavity circuit design.

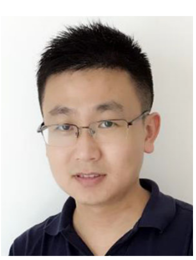

Yang Yang (S'11–M'14–SM'17) was born in Bayan Nur, Inner Mongolia, China, and received the Ph.D. degree from Monash University, Melbourne, VIC, Australia, in 2013.

From 2012 to 2015, he was an Asia Pacific GSP Engineer with Rain Bird. From 2015 to 2016, he was a Senior Research Associate with the Department of Engineering, Macquarie University, Sydney, NSW, Australia. In 2016, he was a Research Fellow with the State Key Laboratory of Millimeter-Waves, City University of Hong Kong. In 2016, he joined the University of Technology Sydney, Australia, as a Lecturer. His research interests include radio-frequency integrated circuits (RFIC), microwave and millimeter-wave circuits and systems, millimeter-wave antennas.

Dr. Yang was the recipient of the CST University Publication Award in 2018, by CST, Germany, and Global GSP Success Award in 2014. He is a currently an Associate Editor for the IEEE ACCESS.

He Zhu received the B.Sc. and M.Eng. degrees from the South China University of Technology, Guangzhou, China, and the Ph.D. degree in electrical engineering from the School of Information Technology and Electrical Engineering, University of Queensland, Brisbane, QLD, Australia.

He is currently a Postdoctoral Research Fellow with Global Big Data Technologies Centre, University of Technology Sydney, Ultimo, NSW, Australia. His research interests include the development of passive and tunable microwave and millimeter-wave devices, radio-frequency-integrated circuits and systems, and beamforming networks for antenna arrays.

Rui-Sen Chen (S'13) was born in Putian, China, in 1989. He received the B.S. degree from the Hunan University of Science and Technology, Hunan, China, in 2012, and the M.E. degree in electromagnetic field and radio technology from the South China University of Technology, Guangzhou, China, in 2015. He is currently working toward the Ph.D. degree with the College of Electronic and Information Engineering, Shenzhen University, Shenzhen, China.

His current research interests include microwave filter, antenna, and cavity circuits.

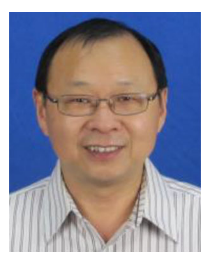

Lei Zhu (S'91–M'93–SM'00–F'12) received the B.Eng. and M.Eng. degrees in radio engineering from the Nanjing Institute of Technology (now Southeast University), Nanjing, China, in 1985 and 1988, respectively, and the Ph.D. degree in electronic engineering from the University of Electro-Communications, Tokyo, Japan, in 1993.

From 1993 to 1996, he was a Research Engineer with Matsushita-Kotobuki Electronics Industries Ltd., Tokyo, Japan. From 1996 to 2000, he was a Research Fellow with the École Polytechnique de Montréal, Montréal, QC, Canada. From 2000 to 2013, he was an Associate Professor with the School of Electrical and Electronic Engineering, Nanyang Technological University, Singapore. He joined the Faculty of Science and Technology, University of Macau, Macau, China, as a Full Professor in 2013, and has been a Distinguished Professor since 2016. From 2014 to 2017, he served as the Head of the Department of Electrical and Computer Engineering, University of Macau. He has authored or coauthored more than 420 papers in international journals and conference proceedings. His papers have been cited more than 5250 times with the H-index of 39 (source: ISI Web of Science). His research interests include microwave circuits, guided-wave periodic structures, planar antennas, and computational electromagnetic techniques.

Dr. Zhu was an Associate Editor for the IEEE TRANSACTIONS ON MICROWAVE THEORY AND TECHNIQUES in 2010–2013 and IEEE MICROWAVE AND WIRELESS COMPONENTS LETTERS in 2006–2012. He served as the General Chair of the 2008 IEEE MTT-S International Microwave Workshop Series on the Art of Miniaturizing RF and Microwave Passive Components, Chengdu, China, and the Technical Program Committee Cochair of the 2009 Asia–Pacific Microwave Conference, Singapore. He served as the member of IEEE MTT-S Fellow Evaluation Committee in 2013–2015 and IEEE AP-S Fellows Committee in 2015–2017. He was the recipient of the First-Order Achievement Award in Science and Technology from the National Education Committee, China, in 1993, Silver Award of Excellent Invention from Matsushita-Kotobuki Electronics Industries Ltd., in 1996, and Asia–Pacific Microwave Prize Award, in 1997.

Yejun He (SM'09) received the Ph.D. degree in information and communication engineering from the Huazhong University of Science and Technology, Wuhan, China, in 2005.

From 2005 to 2006, he was a Research Associate with the Department of Electronic and Information Engineering, The Hong Kong Polytechnic University, Hong Kong. From 2006 to 2007, he was a Research Associate with the Department of Electronic Engineering, Faculty of Engineering, The Chinese University of Hong Kong, Hong Kong. In 2012, he was a Visiting Professor with the Department of Electrical and Computer Engineering, University of Waterloo, Waterloo, ON, Canada. From 2013 to 2015, he was an Advanced Visiting Scholar (Visiting Professor) with the School of Electrical and Computer Engineering, Georgia Institute of Technology, Atlanta, GA, USA. Since 2011, he has been a Full Professor with the College of Information Engineering, Shenzhen University, Shenzhen, China, where he is currently the Director of the Guangdong Engineering Research Center of Base Station Antennas and Propagation, and Shenzhen Key Laboratory of Antennas and Propagation, Shenzhen, China, as well as the Vice Director of Shenzhen Engineering Research Center of Base Station Antennas and Radio Frequency, Shenzhen. He has authored or coauthored more than 100 research papers, books (chapters), and holds approximately 20 patents. His current research interests include wireless mobile communication, antennas and RF.

Dr. He has served as a Technical Program Committee Member or a Session Chair for various conferences, including the IEEE Global Telecommunications Conference, IEEE International Conference on Communications, IEEE Wireless Communication Networking Conference, and IEEE Vehicular Technology Conference. He has served as a Reviewer for various journals, such as the IEEE TRANSACTIONS ON VEHICULAR TECHNOLOGY, IEEE TRANSACTIONS ON COMMUNICATIONS, IEEE TRANSACTIONS ON WIRELESS COMMUNICATIONS, IEEE TRANSACTIONS ON INDUSTRIAL ELECTRONICS, IEEE WIRELESS COMMUNICATIONS, IEEE COMMUNICATIONS LETTERS, IEEE JOURNAL ON SELECTED AREAS IN COMMUNICATIONS, *International Journal of Communication Systems*, *Wireless Communications and Mobile Computing*, and *Wireless Personal Communications*. He is currently serving as an Associate Editor for the IEEE ACCESS and *Security and Communication Networks*. He is a Fellow of IET.